A Wide-Field Spectral Imager

JOHN F. KIELKOPF AND PAMELA M. GRAHAM

Department of Physics, University of Louisville, Louisville, KY 40292; john@aurora.physics.louisville.edu, pam@nimbus.physics.louisville.edu

ABSTRACT. A spectroscopic imager was designed and constructed to provide a new capability for measuring the spectrum of the sky across wide fields of view. The instrument uses a high-speed optical system to form an image on the entrance slit of a matching stigmatic spectrograph, which then disperses a spectrum of a strip of the sky onto a charge-coupled device (CCD). A separate direct imaging system controls pointing and tracking, and both instruments share in tandem a computer-controlled mounting which permits automated data acquisition. The demonstrated optical performance is a 4 Å × 11″ single-pixel resolution in a 4000 Å × 3°.2 field. Absolute calibration on Vega gives a response at 6563 Å that is 7 times the CCD readout noise at an integrated exposure of 1 photon cm^{-2} $Å^{-1}$. Sample airglow, nebular, stellar, and cometary spectra illustrate the detection of extended emission features with fluxes from 5 to 2000 R. A measurement of zenith brightness for Na and Hg emission lines from urban artificial lighting is tabulated.

1. INTRODUCTION

The wide-field spectral imager (WISPI) we describe here was built to measure the emission spectra of extended sources with low surface brightness. Conventional telescopes equipped with nebular spectrographs have such a limited field of view that large-scale structure escapes detection. With this in mind, we designed an instrument specifically for optical spectroscopy with spatial resolution over fields of up to 7°.

Recently a few observational programs have made use of the idea that the detectability of faint extended emission in the night sky is limited not by aperture but by f-ratio (Meaburn 1976). Fast camera lenses, narrowband Hα filters, and charge-coupled device (CCD) detectors combine to give an image field of several degrees with 0°.1 resolution and a sensitivity to 1 R or less (Gaustad et al. 1997; Hentges & McCullough 1998; Gaustad, McCullough, & Van Buren 1996). The Wisconsin Hα Mapper (WHAM) uses a 0.6 m telescope and a Fabry-Perot spectrometer to image the sky in a 1° beam with 12 km s^{-1} velocity resolution in a 200 km s^{-1} spectral window from 4800 to 7200 Å (Reynolds et al. 1998). Integration over the beamwidth and discrimination with high spectral resolution have given detections of high velocity cloud Hα emission lines as faint as 0.06 R (Tufte, Reynolds, & Haffner 1998).

Our interest, however, is to record a comprehensive spectrum and in the same exposure achieve angular resolution of better than 1′ across a field of view of several degrees. Galactic cirrus, for example, is recognizable over fields of several degrees (McCullough 1997; Szomoru & Guhatha-

kurta 1998) but has filamentary structure as small as 30″ (Sandage 1976). Szomoru & Guhathakurta (1998) report that the optical spectroscopic surface brightness of the extended red emission from the diffuse interstellar medium is about 2 orders of magnitude less than the OH night sky emission, which makes its measurement challenging, especially with a narrow field of view. WISPI is a fast imaging system coupled to a long-slit nebular spectrograph and a low-noise detector, designed to observe faint extended sources emitting line spectra. We will describe it briefly here and illustrate its performance with several examples.

2. DESIGN

WISPI can be considered two matched instruments, a front-end imaging system with a stop at the image plane and a stigmatic spectrograph which uses that stop as its entrance slit. Like a "long-slit" spectrograph used with a large telescope, WISPI produces an image which is spatially resolved perpendicular to the direction of dispersion. This concept is constrained by the goal of maintaining the fastest possible optical system throughout. The need for a long physical slit length to give a wide field of view, while optimizing resolution in the two-dimensional image plane, led us to consider using highly corrected transmission optics for the imaging components. Multielement 35 mm photographic camera lenses yield point-source images comparable to the pixel size of typical scientific CCDs. Since they are available with a large selection of apertures and focal lengths, we took advantage of these off-the-shelf com-

ponents in WISPI's design. An overview of the optical layout is shown in Figure 1. It is convenient to explain the factors that led to this arrangement by starting with the detector and working forward, because detector size sets the instrument scale and determines the choice of lenses and grating.

When the instrument was built, the largest low-noise detector we could obtain was a Tektronix 1024 × 1024 thinned, back-illuminated CCD with 24 μm square pixels. Its intrinsic response spans from 3800 Å in the ultraviolet to 11000 Å in the near-infrared, with a peak quantum efficiency of 80% at 7000 Å. Although the detector in WISPI has a proprietary fluorescent overcoating that extends its short-wavelength response to below 2000 Å in the far-ultraviolet, the optical system limits useful response to the band from 4000 to 11000 Å. The detector is mounted in a universal orientation dewar and is cooled by liquid nitro-

gen. Readout electronics are in a separate module, connected to the dewar by a 10 m cable and to a camera control computer by a fast serial link. The packaged detector system used in WISPI was manufactured by Princeton Instruments (now Roper Scientific).

The pixel size and overall dimensions of this detector are matched well to the optical performance of the Nikon ED-IF series of Nikor camera lenses. These employ extra low dispersion (ED) glass, typically in the front elements, and have a mechanically stable internal focus (IF) adjustment. Although they are designed to be used primarily in the visible, our tests of five different samples showed that they are sufficiently well corrected to focus within 2 pixels up to 11000 Å. Although the best focus setting in the blue-violet is shifted from the best setting in the infrared, a band 4000 Å wide may be focused in one image. This bandwidth is an effective compromise between the needs for broad

Nikor lens
400 mm focal length
143 mm diameter

Nikor lens
180 mm focal length
64 mm diameter

Princeton Instruments
1024x1024
CCD

SBIG
320x240
ST5 CCD

Nikor lens
180 mm

Nikor lens
200 mm focal length
100 mm diameter
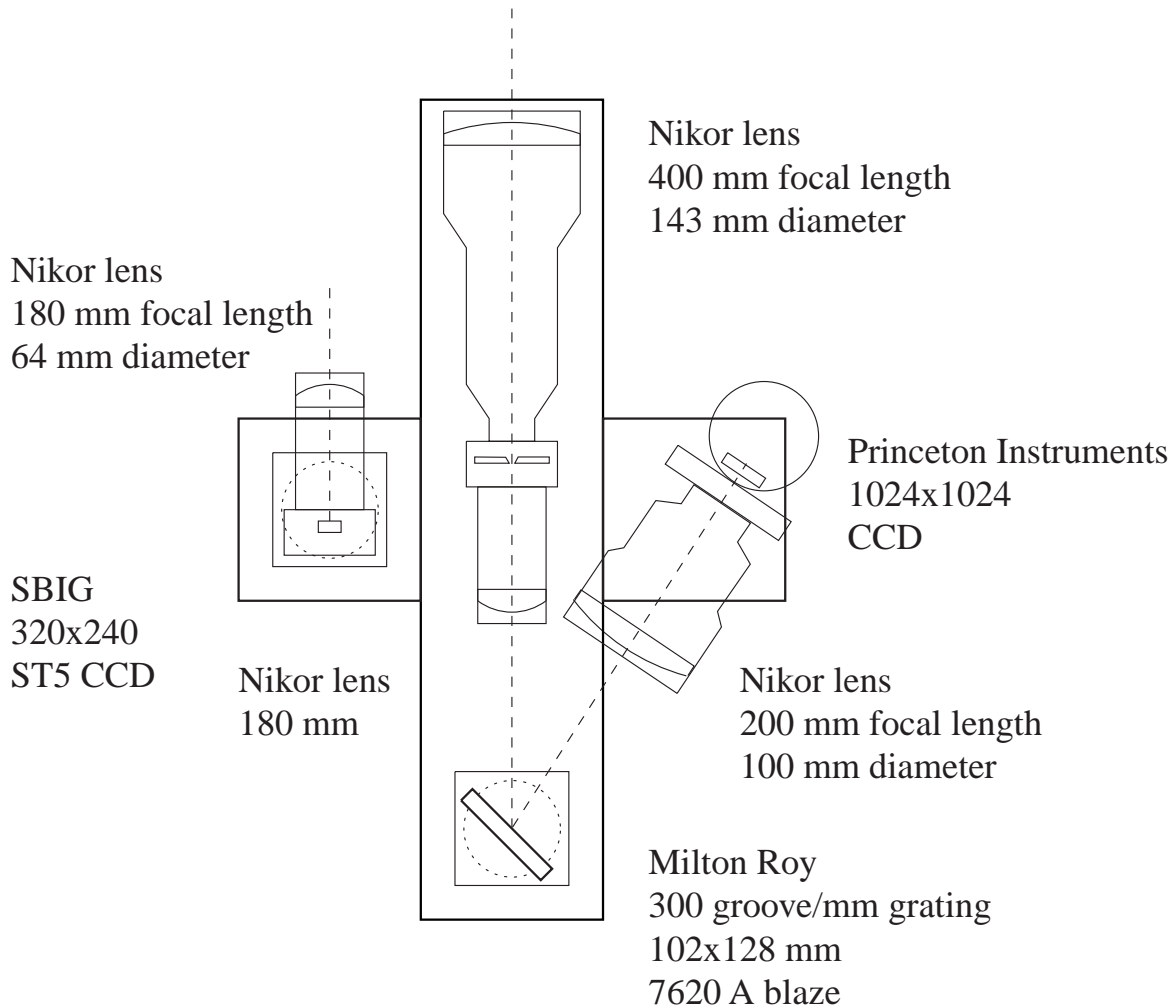
Milton Roy
300 groove/mm grating
102x128 mm
7620 A blaze

FIG. 1.—Optical layout of the Wide-Field Spectroscopic Imager (WISPI). Light enters through the 400 mm focal length f/2.8 objective and forms an image of the sky on the bilateral adjustable slit. It is collimated and then dispersed by a 300 groove mm^{-1} grating. The spectrum and the sky are imaged on the CCD detector.

coverage and for resolution adequate to separate lines in complex spectra. The spectrum from 4000 Å to 11000 Å is covered in two overlapping exposures.

We selected a 200 mm f/2 lens for the spectrograph camera because it was the fastest long focal length lens available of the ED-IF type. It has 10 imaging components protected by an additional flat optical element. In total there are 11 components and 18 air-glass surfaces. The anti-reflection coatings are effective, and we do not notice multiple reflections or serious scattered light in the images. Its mechanical design provides support at a built-in foot near its center of mass and at the standard Nikor lens mount, which makes a bayonet connection to the CCD camera. A focusing ring remains accessible and can be adjusted without disturbing the other system components.

For 1024 pixels along the dispersion direction, the reciprocal dispersion must be approximately 4 Å pixel^{-1}, or 160 Å mm^{-1}, in the spectral image plane to cover 4000 Å. This fixes the ratio of grating groove spacing to the camera focal length, without uniquely determining either one. When a 200 mm focal length lens is used in the spectrograph camera, the desired scale of 4 Å pixel^{-1} is achieved with a 300 groove mm^{-1} grating. We use a 128 mm wide × 102 mm high grating from Milton Roy (formerly Bausch and Lomb, now Spectronic Instruments) with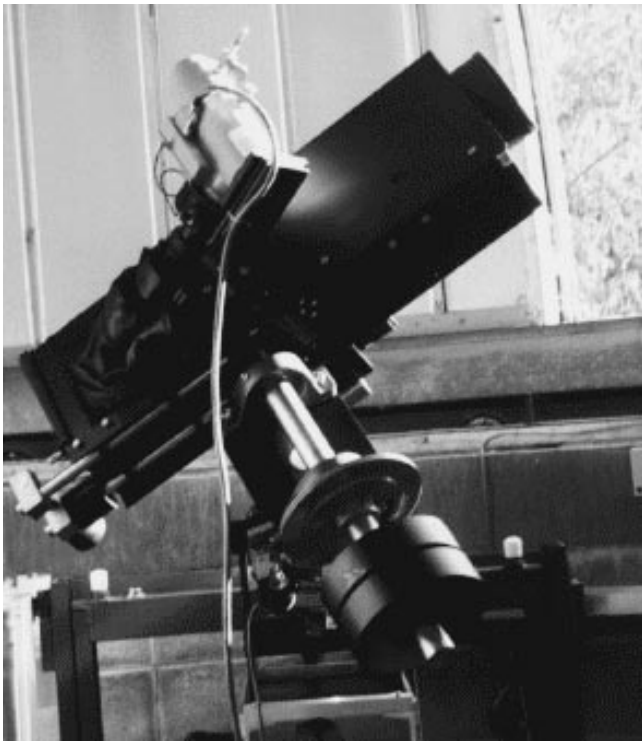 a 7620 Å blaze. The height of the grating is matched to the diameter of the spectrograph camera entrance pupil. The width of the grating is greater than the projected beam diameter. The minimum angle possible between collimator axis and camera axis is 28°, given the sizes of both lenses. The grating is centered on the intersection of the optical axes and mounted on a rotating stage which has a fine adjustment for center wavelength. To preserve final focal-plane image quality, we placed the grating close to the point which makes the spectrograph telecentric on the detector side. The grating has 90% efficiency at its blaze angle, and in first order from 5000 to 11000 Å the response stays above the 50% grating efficiency points.

In diffraction grating instruments such as this one, the first order image at any wavelength contains light from half that wavelength in the second order. When, for example, the spectrograph is to reach a maximum of 10000 Å in the first order, wavelengths less than 5000 Å must be excluded. Combined effects of atmospheric transmission, optical glass transparency, and grating efficiency sharply delimit useful transmission at 4000 Å without a separate filter, so that wavelengths up to 8000 Å may be covered in the first order without an order separation filter. A Wratten 21 gelatin filter with 95% transmission above 5500 Å is inserted in the optical path as a long-pass cutoff filter for imaging above 8000 Å.

Because beam shape changes at the grating, and because the grating sends different wavelengths to the spectrograph camera at varying angles, we require a camera lens of larger diameter than the beamwidth. Since we use an f/2 lens with an aperture of 100 mm as the camera, a smaller 180 mm focal length ED-IF f/2.8 Nikor lens is used for the collimator. The choice of collimator lens was made to optimize coupling between the imaging optics and the spectrograph optics, while providing a roughly 1:1 map of the slit to the

FIG. 2.—The mounted Wide-Field Spectroscopic Imager. The detector dewar is on the near side.
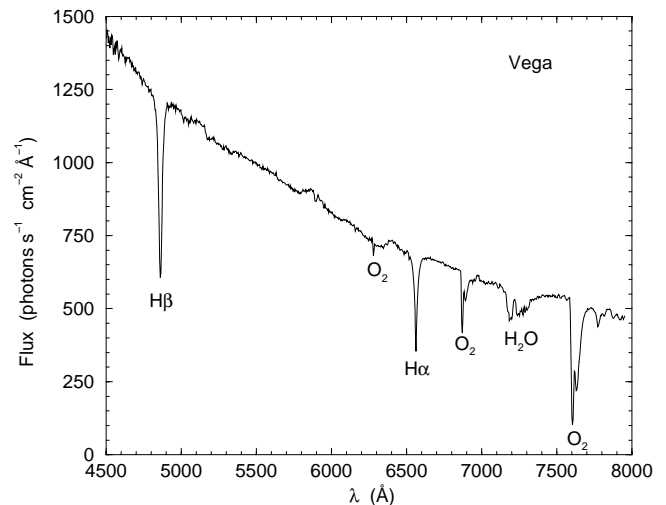

FIG. 3.—A spectrum of Vega recorded in a 10 s exposure on 1997 March 11. The image was processed to remove readout bias, corrected for a flat field, and calibrated against a standard flux for Vega (Tug et al. 1977).
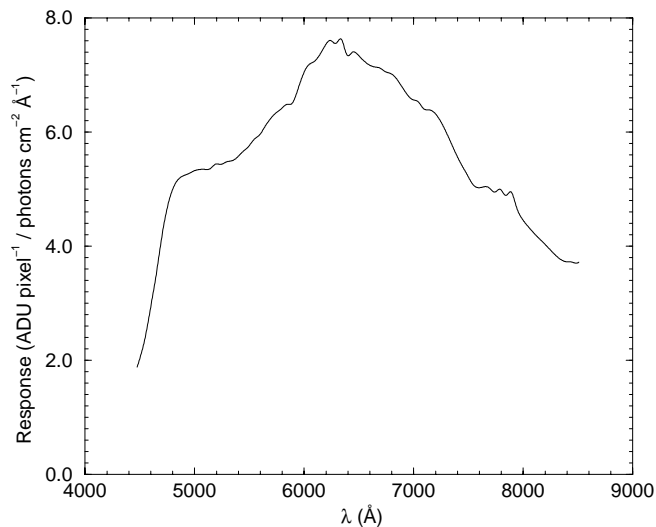
FIG. 4.—Instrumental response derived from spectra of Vega compared to absolute measurements (Tug et al. 1977).

image plane. This lens has eight elements with 12 antireflection-coated air-glass surfaces.

The slit was made by Spex Industries (now Jobin Yvon). It is bilaterally adjustable from 2 μm to 2.5 mm, with a 25 mm height. A machined aluminum cylinder which houses the slit is flanged on each end to accept the bayonet connector of a Nikor lens. To make a rigid coaxial assembly, the collimator and objective lenses are then mounted back to back on opposite sides of the slit, with the collimator supported also by a machined clamp that holds it firmly at its
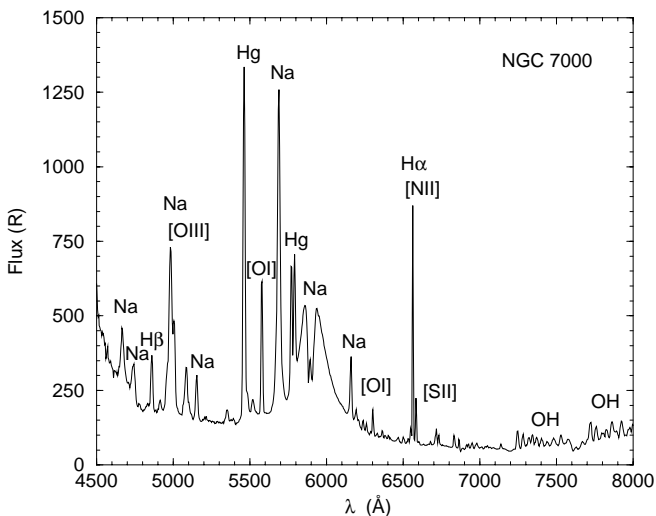

FIG. 5.—Spectrum of the North American Nebula (NGC 7000) also showing airglow and night sky lines derived from an image recorded in a 1200 s exposure on 1997 March 11. This spectrum was extracted through a region showing emission in Hα and has been bias and flat-field corrected and calibrated by comparison to Vega. Typical suburban night sky lines from Na and Hg lighting are indicated and listed in Table 1.
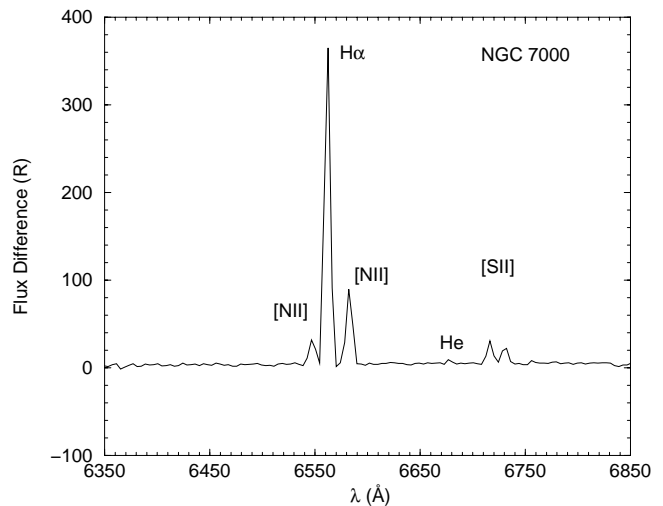

FIG. 6.—Detailed difference spectrum of the North American Nebula with most background features removed. Two regions from the image used to make Fig. 5 were subtracted: one with strong Hα and one with mostly night sky emission. The residual noise is of the order of 1 R.

front element. WISPI's primary structural component consists of this assembly attached to a 20 cm $\times$ 1 m aluminum channel baseplate.

The choice of imaging optics is constrained only in that the lens system must supply an f/2.8 beam over a 25 mm field. An eight-element 400 mm f/2.8 ED-IF Nikor lens gives an image scale of 11″1 pixel^{-1} at the detector and a field of view of 3°2 along the slit. The front two elements are ED glass protected by a flat window so there are a total of nine components with 14 antireflection-coated air-glass surfaces. This 400 mm lens is mounted by a supporting foot close to
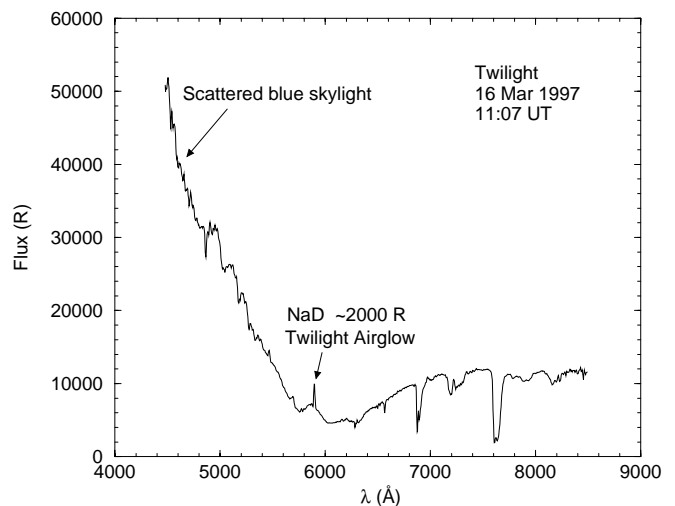

FIG. 7.—Twilight sky spectrum on the morning of 1997 March 16 at 11:07 UT showing the twilight sodium airglow. Telluric absorption lines of O$_2$ and H$_2$O are prominent in the near-infrared, and Rayleigh scattering enhances the blue. The center of the field was 24° above the northeastern horizon at an azimuth of 54°. Sunrise was 44 minutes later at azimuth 92°.
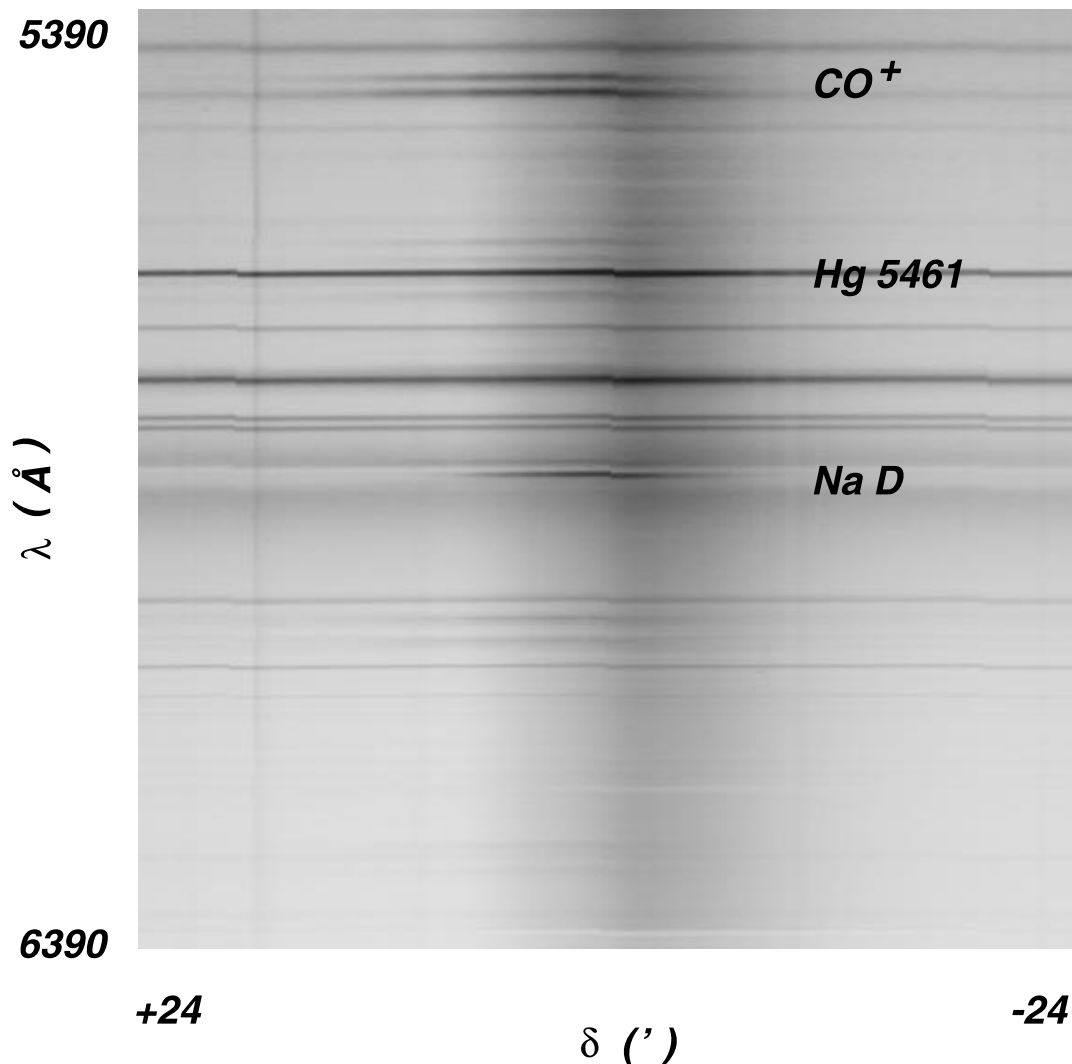
FIG. 8.—Spectral image of comet Hale-Bopp recorded in a 600 s exposure at 01:43 UT on 1997 April 1. This fully corrected image is centered on the Na D lines, and covers a field 1000 Å × 0°8. The Na tail is the prominent emission line indicated, and the dust tail is the vertical continuum down the center of the image.

its center of gravity and the standard camera mount coupled to the slit housing at the rear. A light and dust shield covers the assembled instrument. Much wider fields are accommodated without changing the spectral resolution by substituting the imaging lens for shorter focal lengths. For example, with a 180 mm focal length objective that matches the collimator exactly, the field of view is 7° with a scale of 24″8 pixel^{-1} in the final focal plane.

The telescope is mounted with its slit oriented north-south on a German equatorial. Precision 25 cm diameter 360 tooth worm gears manufactured by Edwin Byers Co. are on both axes. They are driven by Aerotech Unidex microstepping motors programmed for 3600 steps per revolution, or 1″ per step. The motor controllers are serially interfaced to the telescope computer and maintain an accumulated step count which is the offset in arcseconds from a reference position. The controllers are also able to run short programs that are used for tracking. The right ascension program maintains a constant sidereal rate which is increased or decreased in response to a feedback loop from the guiding camera, while the declination program moves the telescope incrementally when declination tracking corrections are needed. The motor controllers operate in response to commands from the telescope computer, but when the telescope is tracking they interact with the guiding camera, directly subject to an interrupt from the telescope controller.

Field acquisition and guiding feedback come from a tandem camera with a Peltier-cooled CCD. The guiding camera platform is attached to the frame of the spectral imager, but it has an adjustable calibrated offset if needed. Normally we use a short focal length camera lens on a
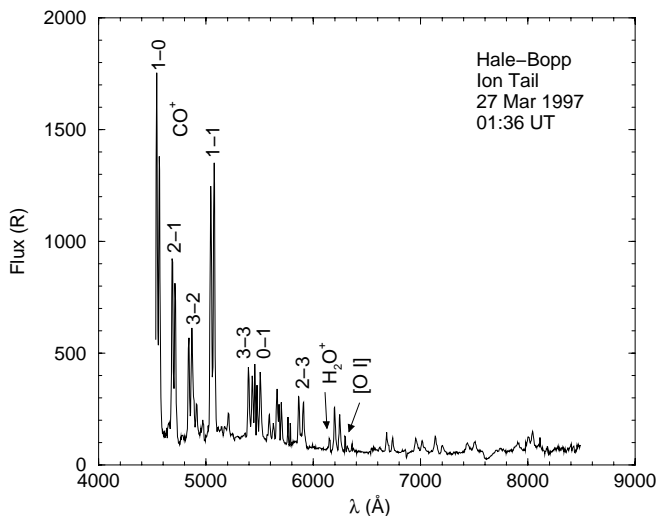
FIG. 9.—Spectrum of comet Hale-Bopp recorded in a 600 s exposure at 01:36 UT on 1997 March 27. The data shown are extracted from the ion tail region with night sky background subtraction and flux calibration on Vega.

Santa Barbara Instrument Group (SBIG) ST-5 camera as the guider. The ST-5 incorporates a Texas Instruments TC255 CCD with 320×240 10 μm square pixels. This is convenient because a lens with a focal length of 180 mm provides 11″5 pixel^{-1}, almost the same angular scale per pixel as the 400 mm lens provides on the spectroscopic CCD. The ST-5 tracking software identifies tracking errors to subpixel accuracy. In this mode the acquisition field is 1°0 × 0°76, smaller than the field of the spectroscopic telescope, but large enough to identify the target. A photograph of the instrument is in Figure 2.

The cameras used by WISPI run on a dedicated Windows 98 or Windows NT system with vendor-supplied software. The camera-control computer uses a Linux system file server and exports its display to remote X-Windows systems using a Virtual Network Computing (VNC) server. VNC is a Java-based utility that enables remote network computers with Java-enabled Web browsers to assume control of remote Windows or Windows NT systems on a TCP/IP network.[1] The WISPI pointing and tracking control is based on a Forth system developed for a 0.5 m telescope (Kielkopf & Hinkle 1987). For the work shown here, it was run with Laboratory Microsystems WinForth on the camera control computer. A WISPI control program for Linux is under development.

---

[1] VNC is free software developed by AT&T Laboratories, Cambridge, and is available from http://www.uk.research.att.com/software.html.

3. PERFORMANCE

While WISPI was designed to study extended sources where its fast optical system is an advantage, it works well on bright stars. The stellar image formed by the objective is of the order of 1 pixel in the final focal plane, and when the slit is open any star imaged within it produces a spectrum. This mode permits a measurement of the throughput without losses at the slit. It is used to produce a flux calibration by comparing the measured spectrum of Vega with the absolute measurement of Tug, White, & Lockwood (1977). This instrumental response calibration may be applied to any stellar spectrum, but a correction for losses at the slit or for tracking error has to be applied when the slit is narrow. A representative flux-calibrated slit spectrum of Vega is shown in Figure 3. The rms noise in this spectrum is of the order of 2 photons s^{-1} cm^{-2} Å^{-1} at 6000 Å where the signal is roughly 800. The instrumental response function derived from Vega is shown in Figure 4, given in units of photons s^{-1} cm^{-2} Å^{-1} above the atmosphere.

The response to a stellar source may be used to transform the signal at each pixel in the spectral image into a flux in rayleighs, where 1 R is 10^6 photons cm^{-2} s^{-1} radiated into all directions by an extended source. As a check, the flux for Hα in the North American Nebula (NGC 7000) is used as an extended source standard (Scherb 1981). A spectrum from that region calibrated in this way is in Figure 5. The observed Hα signal from this image is 800 R above background compared to the value 850 $\pm$ 50 R given by Scherb (1981). The spectrum in Figure 5 appears dominated by other contributions from suburban scattered light at our observing site and from airglow. Airglow at night is well characterized (Chamberlain 1961, p. 345; Roach & Gordon 1973; Allen 1976, p. 134). An atlas at comparable spectral resolution is available (Broadfoot & Kendall 1968), and a detailed high-resolution study of the OH emission spectrum has been made by Osterbrock et al. (1996). The fluxes we observe are consistent with those reported previously and support the calibration of the instrument using Vega.

Table 1 lists for reference the prominent urban lighting night sky lines which we routinely see with their wavelengths and fluxes above the Na continuum. These values were extracted from a zenith exposure on a typical moonless night, recorded at Moore Observatory, an isolated site 22 km from the center of Louisville, Kentucky. All of the observed lines are attributed to Hg vapor and high-pressure Na lamps. Wavelengths for Hg are from the critical compilation of Crosswhite (1972) and for Na are from the wavelength tables of Striganov & Sventitskii (1968, p. 231). Low-pressure Na is not used in this area, and consequently all exposures show the very broad reversed Na D line. The fluxes at the peaks of the broad continuum are given for this line in the table, but most of the line strength is redistributed into the far wings and not represented by this measure-

TABLE 1
URBAN LIGHTING NIGHT SKY SPECTRAL LINES (4490–8500 Å)

Element	λ (Å)	Peak Flux (R)	Comment
Hg......	4816.07	<3	
	5460.73	1140	
	5769.60	440	
	5789.66		
	5790.66	400	Blend
Na......	4494.18		
	4497.66	165	Blend
	4541.63		
	4545.19	<40	Blend
	4664.81		
	4668.56	175	Blend
	4747.94		
	4751.82	105	Blend
	4978.54		
	4982.81	575	Blend
	5148.84		
	5153.40	150	Blend
	5682.63		
	5688.19		
	5688.20	1060	Blend
	5889.95	530	Very broad and reversed blend
	5895.92	525	Very broad and reversed blend
	6154.23		
	6160.75	200	Blend
	7373.23	23	Blend and OH
	7373.49		
	7809.78	15	Blend and OH
	7810.24		
	8183.26		
	8194.79		
	8194.82	145	Blend

(Osterbrock et al. 1992). The weak He line at 7065 Å has a flux of about 0.02 Hα in NGC 7000 but is considerably larger at 0.10 in Orion.

Figure 7 is the spectrum of a dawn twilight clear sky, recorded in a 600 s exposure with the Sun 7°.5 below the horizon at midexposure. The image from which this spectrum was derived is remarkable in the presence of a bright narrow Na D emission. As the calibrated spectrum shows, the flux in this line is of the order of 2000 R above the nearby continuum. This "sodium flash" (Roach & Gordon 1973; Chamberlain 1961, p. 345) occurs when solar radiation is optimal to excite resonance fluorescence from the layer of mesospheric atmospheric Na at an altitude of about 95 km. A laser guide star produced by fluorescence in this layer is a useful reference for adaptive optics imaging (Lloyd-Hart et al. 1998). Spectral images recorded in twilight skies have a background similar to this, although generally much weaker and lacking the sodium flash.

A spectral image of comet C/1995 O1 (Hale-Bopp) in Figure 8 shows $\frac{1}{4}$ of a processed full frame. The slit was oriented north-south, 0°.48 antisunward from the nucleus. Night sky lines run the full width of the image. Emission from the prominent Na tail falls in the reversal dip of the broad urban scattered light profile. The scattered Fraunhofer continuum from the dust tail runs down through the center of the frame, and emission lines of CO^+ ions are strong. This image shows the ability of WISPI to distinguish spatially localized spectral features.

A full spectrum of the ion tail of Hale-Bopp is in Figure 9, where several CO^+ bands and weaker lines of H_2O^+ and [O I] are labeled. Subtraction of the off-tail background in the wide-field image allows detection of features of the order of 5 R in 600 s exposures such as this one.

4. CONCLUDING COMMENTS

The wide-field spectroscopic imager described here has a useful coverage from 4000 to 11000 Å over a 3°.2 field of view with its 400 mm focal length objective. WISPI is best suited for measuring extended emission line sources, but it has the versatility to work well on bright stars. Stellar imaging allows the derivation of an instrumental response function which is then used to transform the raw signal from an extended source to a flux in rayleighs. A calibration on Vega shows that at Hα the instrumental signal is about 7 ADU (compared to a readout noise of 1 ADU) for an incident exposure of 1 photon cm^{-2} $Å^{-1}$ above the atmosphere. Given that the flux in this spectral region from a $V = 0$ star is about 670 photons cm^{-2} $Å^{-1}$ s^{-1}, an 1800 s exposure would produce a signal $10 \times$ readout noise for a $V = 14.8$ star. A 13 R monochromatic object also produces a signal of about 10 ADU in an 1800 s exposure. Objects at the 1 R level are detectable by differencing on- and off-target regions of the same image, with quantitative mea-

ment. The reversed center of the line has a weak secondary central peak which is about 50 R high and to which the airglow Na emission makes a variable contribution, as described below. The D-line wing creates a continuum with significant contributions to the night sky background from about 5500 to 6300 Å. We have not seen other lines due to the buffer gases in these lamps, but emission from Ne, Ar, and possibly Kr also should be present in late twilight as outdoor lighting first turns on.

In spite of the interference from airglow and urban light pollution, very weak features can be extracted by taking the difference of two parts of a single wide-field image. As an example, Figure 6 shows the result of subtracting a region in NGC 7000 in which there is less nebular emission from one where the nebular spectrum is stronger. With careful differencing, the Na continuum disappears, leaving a differential readout noise of the order of 1 R. The usual H II region emission lines are indicated. The observed ratios for the [N II]:Hα:[N II] lines are 0.078:1.00:0.24, about the same as 0.071:1.00:0.21 reported for the Orion Nebula

surements of fainter emission requiring exposures of several hours.

REFERENCES

Allen, C. W. 1976, Astrophysical Quantities (London: Athlone)

Broadfoot, A. L., & Kendall, K. R. 1968, J. Geophys. Res., 73, 426

Chamberlain, J. W. 1961, Physics of the Aurora and Airglow (New York: Academic)

Crosswhite, H. M. 1972, in American Institute of Physics Handbook (New York: McGraw-Hill), 7-29

Gaustad, J. E., McCullough, P. R., & Van Buren, D. 1996, PASP, 108, 351

Gaustad, J., Rosing, W., Chen, G., McCullough, P., & Van Buren, D. 1997, BAAS, 190, 30.05

Hentges, P. J., & McCullough, P. R. 1998, BAAS, 192, 40.05

Kielkopf, J. F., & Hinkle, S. 1987, PASP, 99, 442

Lloyd-Hart, J., et al. 1998, ApJ, 493, 950

McCullough, P. R. 1997, AJ, 113, 2186

Meaburn, J. 1976, Detection and Spectrometry of Faint Light (Dordrecht: Reidel)

Osterbrock, D. E., Fulbright, J. P., Martel, A. R., Keane, M. J., & Trager, S. C. 1996, PASP, 108, 277

Osterbrock, D. E., Tran, H. D., & Veilleux, S. 1992, AJ, 389, 305

Reynolds, R. J., Hausen, N. R., Tufte, S. L., & Haffner, L. M. 1998, ApJ, 494, L99

Roach, F. E., & Gordon, J. L. 1973, The Light of the Night Sky (Dordrecht: Reidel)

Sandage, A. 1976, AJ, 81, 954

Scherb, F. 1981, ApJ, 243, 644

Striganov, A. R., & Sventitskii, N. S. 1968, Tables of Spectral Lines of Neutral and Ionized Atoms (New York: Plenum)

Szomoru, A., & Guhathakurta, P. 1998, ApJ, 494, L93

Tufte, S. L., Reynolds, R. J., & Haffner, L. M. 1998, ApJ, 504, 773

Tug, H., White, N. M., & Lockwood, G. W. 1977, A&A, 61, 679